Magnetic phase transitions in irradiated haematite

1992 J. Phys.: Condens. Matter 4 7839

(http://iopscience.iop.org/0953-8984/4/38/014)

J. Phys.: Condens. Matter 4 (1992) 7839–7850. Printed in the UK

Magnetic phase transitions in irradiated haematite

Ö F Bakkaloğlu, O Nikolov† and M F Thomas
Department of Physics, University of Liverpool, Liverpool L69 3BX, UK

Received 27 April 1992, in final form 2 July 1992

Abstract. In haematite the magnetic phase change from a weak ferromagnetic state to an antiferromagnetic state that occurs as the temperature is decreased through the critical value is known as the Morin transition. The different magnetic states give rise to distinct Mössbauer spectra and this technique was used to study the phase changes in samples of haematite that had been exposed to different levels of neutron irradiation. At relatively low levels of irradiation the normal Morin transition was observed at a temperature lower than that for non-irradiated haematite. In samples with higher levels of irradiation, as the temperature was decreased, the normal weak ferromagnet to antiferromagnet transition occurred, but on further decrease of temperature a reverse phase transition was observed back to the weak ferromagnetic state. The magnetic phase transitions occurring in all the irradiated samples were studied and the critical temperatures measured. The mechanism and conditions required for the normal and reverse Morin phase transitions are discussed in terms of a model of competing single-ion and magnetic dipole anisotropy energy. It is found that the model can account for the sequences of transitions and the critical temperatures. The nature of the transitions is seen to be a mixture of first and second order.

1. Introduction

A magnetic phase transition in haematite, detected by magnetic susceptibility measurements by Morin [1], was shown by the neutron diffraction study of Shull *et al* [2] to consist of a transition between the high-temperature weak ferromagnetic phase and the low-temperature antiferromagnetic phase illustrated in figure 1. It was seen that in the antiferromagnetic phase the Fe^{3+} spins lie along the [111] trigonal axis while in the weak ferromagnetic phase the spins lie in a plane normal to this axis and they are canted to produce a weak ferromagnetic moment. In a number of studies, typified by [3], it has been shown that the transition temperature T_M is sensitive to small amounts of impurities but a typical value of T_M obtained using a high-purity manufactured crystal of haematite, grown in a flux of $Na_2B_4O_7$ is $T_M = 252$ K with a transition width of 12 K [4]. The Néel temperature of haematite has been measured as $T_N = 948$ K [3].

In two recent studies on neutron-irradiated samples of haematite [5, 6] it has been reported that decreasing temperature shows the normal Morin transition to be followed at lower temperature by a reverse transition which largely restores the weak ferromagnetic phase. This investigation was undertaken to re-examine such samples using Mössbauer spectroscopy which, in addition to detecting the magnetic phase transitions, is sensitive to the nature or order of the phase changes.

† Permanent address: Institute of Nuclear Research, Sofia, Bulgaria.

0953-8984/92/387839+12$04.50

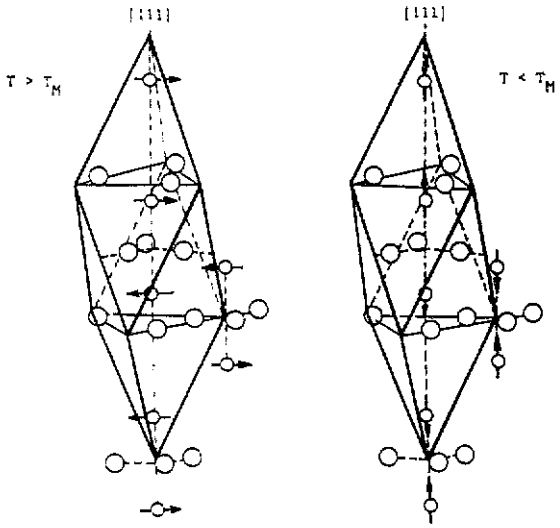

Figure 1. Crystallographic and magnetic structures of haematite. The high-temperature weak ferromagnetic phase is shown on the left with the Fe^{3+} spins lying on the basal (111) plane, canted slightly from antiparallel alignment to give a weak ferromagnetic state. The low-temperature antiferromagnetic phase is on the right with the Fe^{3+} spins ordered along this trigonal axis.

2. Experimental technique

Five samples were used in the study, the control, non-irradiated sample was of the previously described high-purity haematite [4]. The other four samples were of the same haematite material but were subjected to different degrees of irradiation from the neutron flux of a reactor. The degree of irradiation of each sample is characterized by the fraction of atoms displaced (FODA) defined by the expression [7]

$$\text{FODA} = \int \frac{\phi(E)\sigma_s(E)t\,dE}{AE_d}$$

where $\phi(E)$ and $\sigma_s(E)$ are the neutron flux and the elastic scattering cross section at the neutron energy E, A and E_d are the relative atomic mass and the displacement energy of the atoms in the sample and t is the time of irradiation. The FODA values of the irradiated samples are listed in table 1.

Table 1. Comparison of the experimental and theoretical magnetic phase transition temperatures. The experimental values were taken as the temperatures for which the quadrupole shift $\Delta = 0$; the theoretical values were taken from the crossings of the curves of figure 5.

Sample	FODA	Experimental		Theory		
		T_{M1}(K)	T_{M2}(K)	T_{M1}(K)	T_{M2}(K)	$B_{si}(0)/B_{md}(0)$
Control	0.0	255 ± 2				
1	0.0009	227 ± 2		224 ± 5		1.006
2	0.0012	227 ± 2		228 ± 5		1.006
3	0.0020	195 ± 2	80 ± 2	194 ± 5	93 ± 5	0.99
4	0.0022	165 ± 2	120 ± 2	163 ± 5	133 ± 5	0.99

Mössbauer spectra were taken by using a ^{57}Co in Rh source of initial strength 100 mCi with conventional transmission geometry using a double-ramp waveform to give a flat background for the absorption spectra. The spectrometer was calibrated at room temperature with an α-Fe foil of thickness 25×10^{-3} mm. Isomer shifts are measured relative to this standard. The temperature for each spectrum is selected and maintained by a liquid helium flow cryostat. The sample temperature is monitored by a semiconductor resistance thermometer mounted on the sample block which showed that the temperature remained stable at the chosen value to within 0.1 K over the counting time of a few hours.

3. Results and analysis

Mössbauer spectra were taken over the temperature range of 4.2 K to 290 K in $\simeq 20$ K steps for all samples. It was found that reasonable fits to all the data could be obtained with two magnetic sextet components. Examples of the spectra and fits are shown in figure 2 where the spectra span the phase transition temperature range for sample 3. These spectra show directly that at the ends of the temperature range, 4.2 K and 290 K, the splitting Δ_{12} between the low velocity lines 1 and 2 exceeds the splitting Δ_{56} between the high-velocity lines 5 and 6 giving rise to a negative quadrupole shift. However, in the 130 K spectrum Δ_{12} is less than Δ_{56} showing a positive quadrupole shift. In this way the normal and reverse Morin transitions can be seen directly in this sequence of spectra.

Mean values of quadrupole shift Δ defined as

$$\Delta = \tfrac{1}{2}(\Delta_{12} - \Delta_{56})$$

were calculated from those of the fitted components, weighted by relative absorption intensity. The justification for this definition of quadrupole shift Δ is given in [8] where Δ is equivalent to the quantity -2ϵ. The variation of quadrupole shift with temperature for the irradiated samples is compared with that for the control sample in figure 3. The phase transitions are clearly seen in these graphs. For the control sample, as the temperature is decreased, the weak ferromagnetic phase, characterized by a quadrupole shift value of -0.21 mm s^{-1} changes at $T_{M1} = 255 \pm 2$ K to the antiferromagnetic phase whose observed quadrupole shift of $+0.42$ mm s^{-1} matches the theoretical expectation. In the two most lightly irradiated samples 1 and 2 the normal Morin transition is observed. However, for these samples the transition temperature, taken at $\Delta = 0$, is reduced to 227 ± 2 K. There are also indications that some weak ferromagnetic phase may persist below the Morin transition as the quadrupole shift below the transition temperature never attains the value of $+0.42$ mm s^{-1} and shows a decrease to $\simeq 0.34$ mm s^{-1} below 60 K.

The most dramatic behaviour is seen in the more heavily irradiated samples. In sample 3 the normal Morin transition is observed at a temperature of 195 ± 2 K but, on further reduction of temperature a reverse transition is seen at 80 ± 2 K. At temperatures below 280 K it appears that there may be coexistence of phases as the largest value of quadrupole shift, observed at 130 K, is $+0.25$ mm s^{-1} and at 4.2 K the value has decreased only to -0.18 mm s^{-1}. However, it is clear that in the majority of this sample there has been a normal Morin transition at $T_{M1} = 195 \pm 2$ K and a reverse Morin transition at $T_{M2} = 80 \pm 2$ K. A more extreme version of this process is

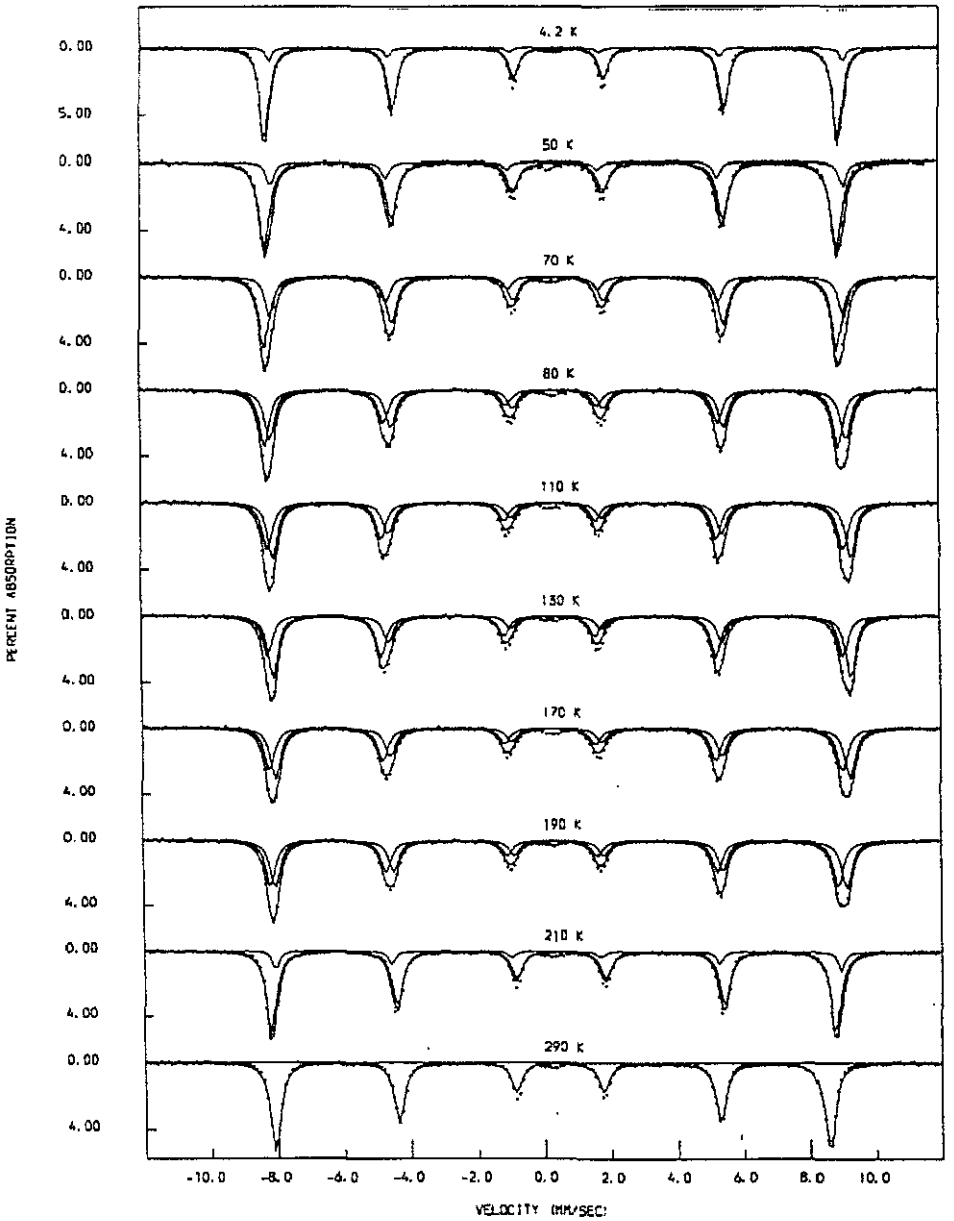

Figure 2. A sequence of Mössbauer spectra taken over the temperature range 4.2 K to 290 K on the irradiated sample 3. The spectra are seen to be magnetic sextets; we associate numbers 1 to 6 with these lines in order of increasing velocity. The data show a change from negative quadrupole shift at 4.2 K to positive quadrupole shift at 130 K and back to negative quadrupole shift at 290 K. The spectra are fitted with two magnetic sextet components.

seen with sample 4 where the Morin and reverse Morin transitions, as defined above, are seen to occur at $T_{M1} = 166 \pm 2$ K and $T_{M2} = 120 \pm 2$ K respectively. In this case while the weak ferromagnetic phase appears to be nearly pure at temperatures

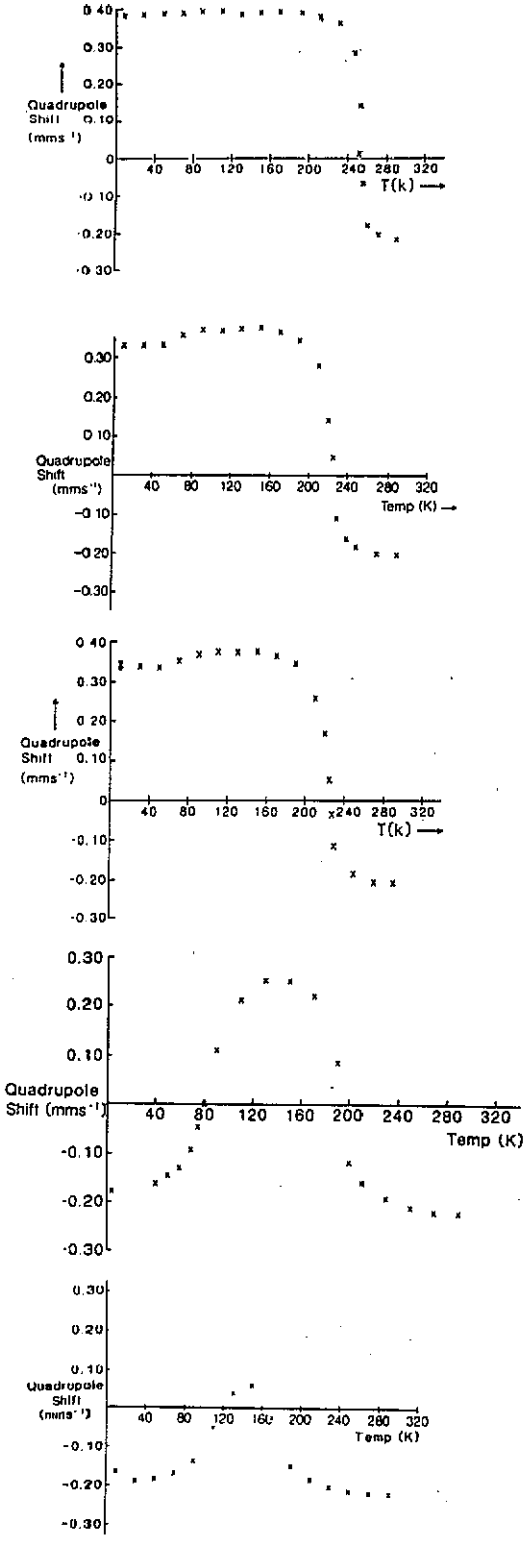

Figure 3. Graphs showing the variation of quadrupole shift Δ with temperature for the control and irradiated samples. The sequence is the control sample at the top then in order downwards samples 1, 2, 3 and 4. It is seen that the control sample and samples 1 and 2 show only the normal Morin transition while samples 3 and 4 show normal and reverse Morin transitions. The evaluation of Δ is described in the text and the experimental values of the transitions are obtained from these graphs where $\Delta = 0$.

$T > 280$ K and $T < 50$ K the state of the sample for $120\,\text{K} < T < 166$ K where Δ is positive but has a maximum value of only 0.08 mm s^{-1} indicates considerable phase coexistence.

In the sequences of spectra shown the temperature was increased from 4.2 K to room temperature. Separate sets of measurements were taken with increasing and decreasing temperature around the transition points to investigate possible hysteresis. In no case was significant hysteresis observed.

Values of the magnetic hyperfine field B_{hf} were obtained from weighted averages of the fitted sextets and the variation of B_{hf} with temperature for all samples is shown in figure 4. The shapes of these graphs give visual confirmation of the phase changes as the higher hyperfine field associated with the antiferromagnetic phase is evident in temperature ranges that match the changes of quadrupole shift. The identifiable increase in B_{hf} due to the antiferromagnetic phase in the graph for sample 3 allows an evaluation to be made of the dipolar component B_{dip} of the hyperfine field. While the dominant contribution to the total hyperfine field from the Fermi contact term is isotropic, the dipolar component has an angular variation that can be expressed as

$$B_{dip}(3\cos^2\theta - 1)/2$$

where θ is the angle between the Fe^{3+} spins and the principal axis of the electric field gradient tensor which is the [111] axis. Thus the hyperfine field in the antiferromagnetic phase contains a component $+B_{dip}$ while in the weak ferromagnetic phase, where the spins are at an angle $\theta = 90°$ to the (111) axis, the dipolar contribution is $-\frac{1}{2}B_{dip}$. From the graph for sample 3 in figure 4 the increase in the hyperfine field due to the antiferromagnetic phase component is 6.5 ± 0.7 kG. This enables the dipolar component of the hyperfine field to be evaluated as

$$B_{dip} = \tfrac{2}{3}6.5\ 1/0.73 = 6.0 \pm 0.6\ \text{kG}$$

where the factor $\frac{2}{3}$ scales the relative change from antiferromagnetic to weak ferromagnetic phase and the factor $1/0.73$ is a correction for the purity of the antiferromagnetic phase which is estimated from the value of the quadrupole shift.

4. Discussion

The topics considered in this section are the cause of the reverse Morin transition observed in the more heavily irradiated samples of haematite and the nature or order of the observed magnetic phase transitions.

4.1. Mechanism for the magnetic phase transitions

The normal Morin transition, observed at $T_M \simeq 260$ K in pure bulk haematite has been explained [9] on the basis of competition between two separate terms of anisotropy energy. At low temperature the single-ion anisotropy of the Fe^{3+} ions is dominant, stabilizing the antiferromagnetic phase but at high temperature the magnetic dipolar anisotropy energy dominates which favours the weak ferromagnetic phase. The Morin transition occurs at the temperature T_{M1} where the magnitudes of single-ion and magnetic dipolar anisotropy energy become equal. For the normal Morin transition to occur the zero-temperature single-ion anisotropy

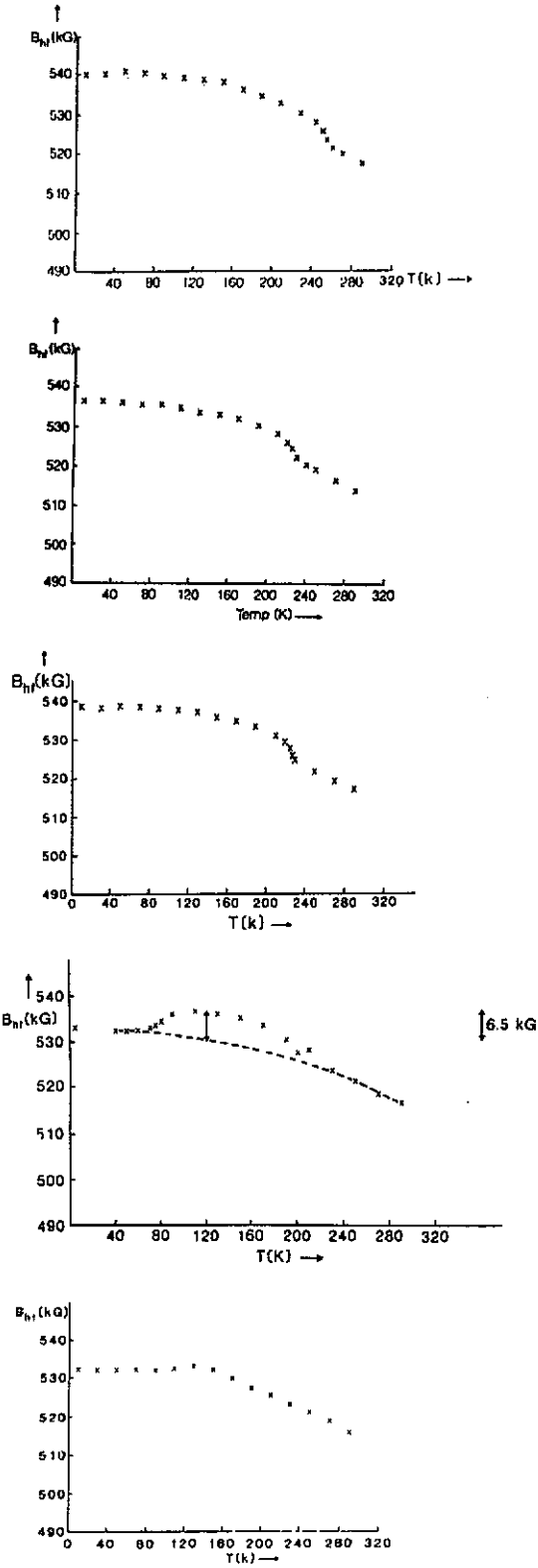

Figure 4. Graphs of the variation of hyperfine field with temperature for the control and irradiated samples. The sequence from top to bottom of control then samples 1, 2, 3 and 4 is the same as in figure 3. The magnetic phase changes are visible in these graphs through the increased magnetic hyperfine field of the antiferromagnetic phase. The cause of this increase, the dependence of the magnetic dipole component on the direction of the spins to the trigonal axis, is evaluated in the text from the observed increase in the graph of sample 3.

field $B_{si}(0)$, related to the zero-temperature single-ion anisotropy energy $K_{si}(0)$ by $B_{si}(0) = K_{si}(0)/g\mu_B$ where $g = 2$ for the Fe^{3+} ion and μ_B is the Bohr magneton, must be greater than the zero-temperature magnetic dipolar anisotropy field $B_{md}(0) = -K_{md}(0)/g\mu_B$. At temperatures $T > 150$ K, B_{si} decreases faster than B_{md} resulting in the crossing of the graphs of B_{si} versus T and B_{md} versus T which drives the normal Morin transition.

Expressions for the variation with temperature of B_{si} and B_{md} have been calculated on the basis of the molecular field approximation by Yoshida [10], Tachiki and Nagamiya [11] and Artman *et al* [9]. Using the notation of the latter authors the anisotropy fields at temperature T can be written as

$$B_{si}(T) = B_{si}(0)[2(S+1) - 3B_s(z)\coth(z/2S)]/(2S-1)$$

$$B_{md}(T) = B_{md}(0)B_s^2(z)$$

where $B_{si}(0)$ and $B_{md}(0)$ are the magnitudes of the single-ion and magnetic dipolar anisotropy fields at 0 K, $S = \frac{5}{2}$ is the spin of the Fe^{3+} ions, $B_s(z)$ is the Brillouin function whose argument $z = g\mu_B S\lambda M/kT$. In this latter expression M is the sublattice magnetization, λ the molecular field constant, and k is the Boltzmann constant.

The temperature dependencies of the anisotropy fields are contained in the factor z—both explicitly in kT and implicitly in the sublattice magnetization M. Values of the magnetization at temperature T, $M(T)$ and hence of z were obtained from the saturation magnetization $M(0)$ via the relationship

$$M(T) = M(0)B_{hf}^c(T)/B_{hf}^c(0)$$

where B_{hf}^c represents the component of the hyperfine field due to the Fermi contact term. Experimental data were used for the values of B_{hf}^c. This evaluation of $M(T)$ is justified by the relationship that the dominant contact term of the hyperfine field is accurately proportional to the sublattice magnetization. Experimental values of B_{hf} were corrected for the small known contribution of the dipolar term B_{dip} to obtain the required values of B_{hf}^c.

With the temperature variation of $B_{si}(T)$ and $B_{md}(T)$ defined by the expressions above the single adjustable parameter that affects the crossing of the curves is the value of $B_{si}(0)/B_{md}(0)$. In order to account for the Morin transition temperature in pure bulk haematite a ratio $B_{si}(0)/B_{md}(0) = 1.006$ is required [9]. In figure 5 are shown graphs of B_{si} versus T and B_{md} versus T for all the irradiated samples in which $B_{si}(0)/B_{md}(0)$ has been adjusted to give best agreement with the observed temperatures of the magnetic phase transitions. The values of temperatures predicted for the phase transitions by the procedure described above are compared with the experimental values in table 1 which also lists the values of $B_{si}(0)/B_{md}(0)$ adopted for each sample.

It is seen that for values of $B_{si}(0)/B_{md}(0) \geqslant 1$ a single crossing of the curves occurs corresponding to the normal Morin transition. For values of $B_{si}(0)/B_{md}(0) < 1$, however, double crossing of the curves can occur corresponding to the sequence of normal and reverse Morin transitions occurring at the temperatures T_{M1} and T_{M2} that are listed in table 1. A further decrease in $B_{si}(0)/B_{md}(0) < 1$ can be seen to result in no crossing of the curves corresponding to a prediction of no magnetic

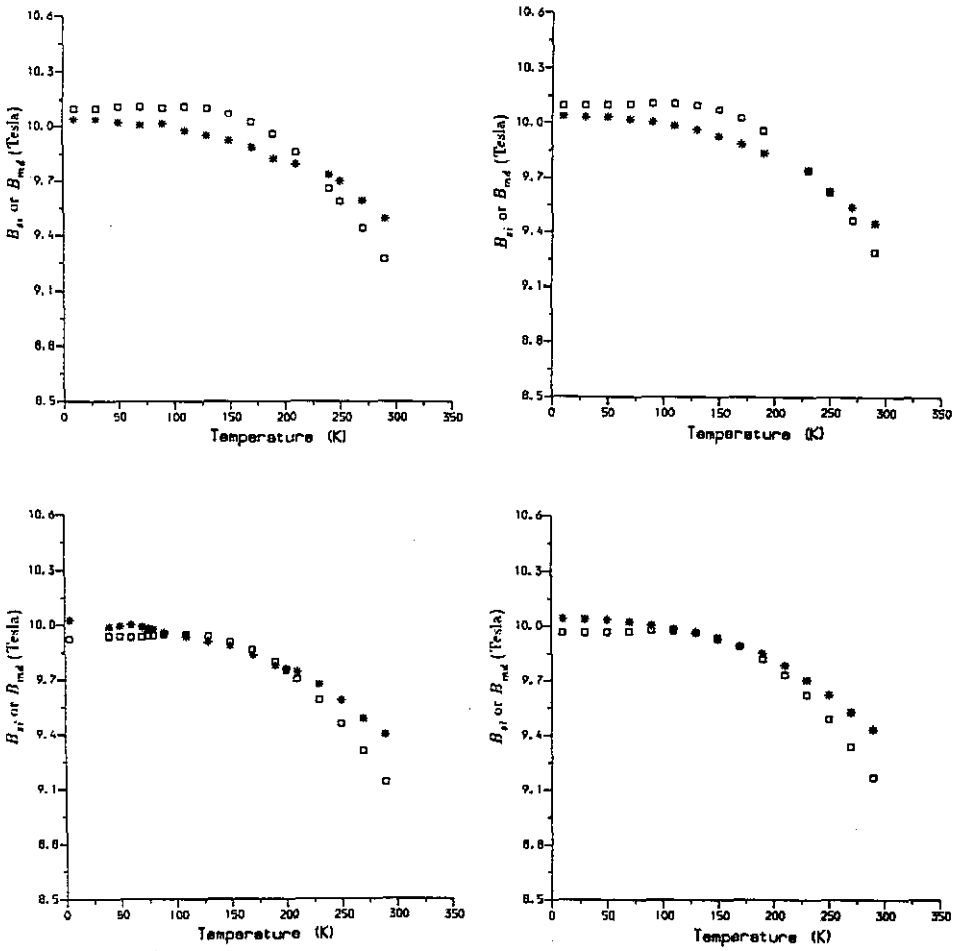

Figure 5. Calculated variation of B_{si} (as □) and B_{md} (as *) with temperature for all irradiated samples. The sequence is top, left to right samples 1 and 2 and bottom left to right samples 3 and 4. The expressions and method of evaluation are described in the text. Magnetic phase transitions are predicted when these curves cross. It is seen that for samples 1 and 2 a single crossing occurs predicting the normal Morin transition. For samples 3 and 4 two crossings of the curves are indicated predicting normal and reverse Morin transitions.

phase transitions and the persistence of the weak ferromagnetic phase throughout the temperature range.

In order to account for our experimental results it appears that increased radiation damage has the effect of decreasing the ratio $B_{si}(0)/B_{md}(0)$. The Morin transition is such a sensitive balance between competing anisotropy terms that it is not surprising that small disruptions in the lattice of magnetic ions such as that provided by impurity ions or by neutron irradiation can cause large modifications in Morin transition temperature or even the reverse Morin transition observed in this study.

4.2. Nature of the magnetic phase changes

In this section we review the experimental evidence to investigate whether the magnetic phase transitions proceed by an abrupt change between antiferromagnetic and

weak ferromagnetic phases or by a continuous transition. In the former case, first-order phase change, as the temperature is varied through the critical region the transition would occur by changing proportions of the antiferromagnetic and weak ferromagnetic phases. Coexistence of phases and possibly hysteresis can occur close to the transition temperature. In the latter case, second-order phase change, as the temperature is varied the transition would proceed by the spins rotating continuously. In this case there should be no phase coexistence or hysteresis. Analyses of the Mössbauer spectra in the critical temperature ranges give information on the nature of the phase changes.

Pure haematite appears to have the first-order phase transition [9, 12]. There is some evidence that impurities cause a third component in haematite supporting a possible mixing of second-order nature in the Morin transition [13]. Neutron irradiation was expected to introduce irregularities into the lattice that could affect the nature of this phase transition.

As presented above reasonable fits to the spectra at all temperatures have been obtained using two magnetic sextet components. If these components could have been unambiguously identified with antiferromagnetic and weak ferromagnetic phases by fixing their quadrupole shifts at $+0.42$ mm s^{-1} and -0.21 mm s^{-1} respectively and the fits achieved simply by change of relative intensity as the temperature is varied through the critical range, then the mechanism would have been clearly shown to be of first order. However, in order to obtain good fits with two sextet components near the transition temperatures, the values of quadrupole shifts in both components had to be left to vary. The fits then required that for each magnetic component the magnitude of the quadrupole shift decreased as the temperature approached the critical value. Thus the transitions do not proceed by pure first-order mechanism.

Alternatively it was not possible to fit the experimental spectra well in the critical temperature range with a single sextet whose value of quadrupole shift varied continuously from the antiferromagnetic phase value to that of the weak ferromagnetic phase as would be required for a pure second-order transition.

A final series of fits were made with three sextet components. Two of the components had their values of quadrupole shift fixed at $+0.42$ mm s^{-1} and -0.21 mm s^{-1}, characteristic of antiferromagnetic and weak ferromagnetic phases respectively. The quadrupole shift of the third component was allowed to vary. This approach gave fits that were slightly but significantly better than the fits with the two sextets having free values of quadrupole shift. An example of this improvement is shown in figure 6 where the extended scale is necessary to demonstrate the better fit. The values assumed by the quadrupole shift, and hyperfine field, of the third component were always between those of the antiferromagnetic and weak ferromagnetic phases and varied smoothly through the critical temperature ranges consistent with the rotation of spins between the [111] axis and the plane normal to this axis. Thus the third component may be envisaged as due to a fraction of the spins that rotate continuously from the [111] axis to the (111) plane as the temperature is varied through the transition region. The variation of the relative intensity of this third or intermediate component with temperature is shown for samples 1 and 3 in figure 7. It is seen that the intensity is peaked at the phase transition temperatures though, in sample 3, there is appreciable intensity of this component throughout the temperature interval 70 K–200 K and in sample 1 the component appears at the lowest temperatures. Interpreting these graphs it appears that a large proportion of the phase changes proceeds continuously through the intermediate component but since the relative intensity of this compo-

nent falls well short of 100% even at the transition temperatures, an appreciable proportion of the phase transitions has first-order character. It thus appears that in these samples first- and second-order phase changes occur simultaneously.

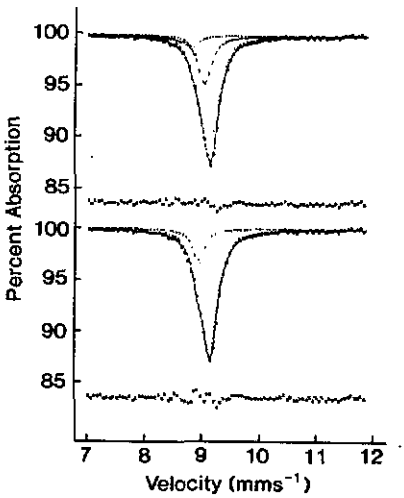

Figure 6. An illustration of the better fit obtained using three rather than two magnetic sextet components. An extended scale is necessary to demonstrate the improved fit which is on sample 1 at 215 K.

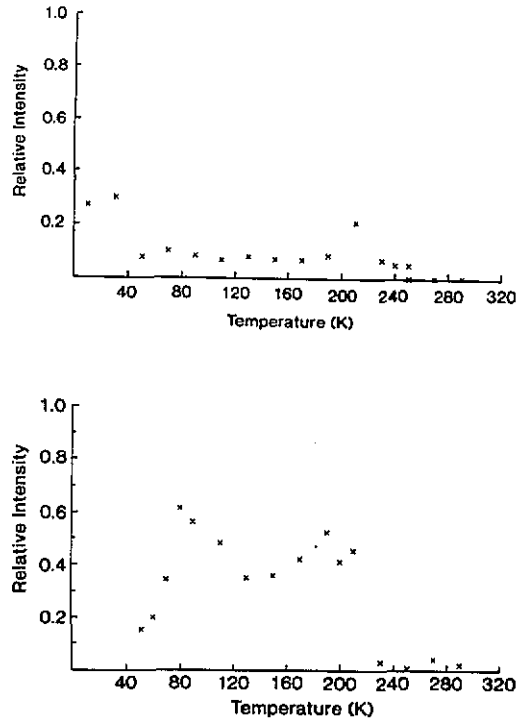

Figure 7. Graphs showing the variation of relative intensity with temperature of the intermediate magnetic component in the three component fits described in the text. The graphs are for (top) sample 1 and (bottom) sample 3. It is seen that the relative intensity of this component is maximum at the magnetic phase transitions and that for sample 3 it has appreciable intensity throughout the temperature range 70 K to 200 K.

Parametrizing the total anisotropy energy K as

$$K = K_1 \sin^2\theta + K_2 \sin^4\theta$$

it has been shown that, for a phase transition occurring when $K_1 = 0$, the nature of the phase change depends upon the sign of K_2. For $K_2 < 0$ the phase change is of first order while for $K_2 > 0$ the change is of second order. The observed results indicate that the radiation damage caused by neutron bombardment creates inhomogeneity in the samples with some regions having K_2 positive and others negative. This occurs even at the relatively low dose applied to sample 1. Increased radiation damage not only changes the relative magnitudes of the single-ion and magnetic dipole contributions to K_1 as discussed in the previous section, but in sample 3

causes coexistence of the intermediate phase and weak ferromagnetic phase over large temperature ranges.

5. Conclusions

The Morin transition is known to be a sensitive balance between competing terms of magnetic anisotropy. This work shows that radiation damage caused by neutron irradiation can change the relative magnitudes of the competing single-ion and magnetic dipolar terms and hence cause different sequences of magnetic phase changes occurring at different critical temperatures. More subtly the nature of the phase changes can be affected and, due to inhomogeneities in the damage, the transitions can proceed by different mechanisms simultaneously within the same sample.

Acknowledgments

ÖFB wishes to acknowledge the support of a grant from Atatürk University, Turkey, throughout this work. ON is grateful for the support of an award from the University of Liverpool. The work was financially supported by the SERC.

References

[1] Morin F J 1950 *Phys. Rev.* **78** 819
[2] Shull C G, Stanser W A and Wollan E O 1951 *Phys. Rev.* **83** 333
[3] Besser P J, Morrish A H and Searle W 1967 *Phys. Rev.* **153** 632
[4] Pankhurst Q A, Johnson C E and Thomas M F 1986 *J. Phys. C: Solid State Phys.* **19** 7081
[5] Zhetbaev A K and Donbaev K M 1986 *Hyperfine Interact.* **28** 623
[6] Zhetbaev A K and Donbaev K M 1990 *Phys. Status Solidi* b **157** 55
[7] Glasstone S and Sesonshe A 1981 *Nuclear Reactor Engineering* (New York: Van Nostrand) p 441
[8] Fritzsch E, Pietzsch C, Heegn H and Huhn H-J 1982 *Cryst. Res. Technol.* **17** 1443
[9] Artman J O, Murphy J C and Foner S 1965 *Phys. Rev.* **138** A912
[10] Yoshida K 1951 *Prog. Theor. Phys. (Kyoto)* **6** 691
[11] Tachiki M and Nagamiya T 1958 *J. Phys. Soc. Japan* **13** 452
[12] Levinson L M, Luban M and Shtrikman S 1969 *Phys. Rev.* **187** 715
[13] Gangas N-H J, Bakas T and Moukarika A 1985 *Hyperfine Interact.* **23** 245